Discriminating models of meson structure using global QCD fits

Brief remarks for the workshop discussion

Aurore Courtoy,[1] Tim Hobbs,[2] Fred Olness,[2] Pavel Nadolsky[2]

[1]UNAM, Mexico [2]SMU, USA

Based on studies with CTEQ-TEA, nCTEQ, and xFitter collaborations

Key lesson from 35+ years of global fits of nucleon and nuclear PDFs:

Complete error analysis, including all sources of uncertainties, is critical for falsifying theoretical models using experimental data

My apologies for incomplete references!

CTEQ

Are any of these pion models ruled out? Not so fast…

- Nambu and Jona-Lasinio Model:
  - R. Davidson, E. Arriola, PLB (1995)
  - J.T. Londergan *et al.* PLB (1994).
  - T. Shigetani *et al.* PLB (1993).
- Dyson Schwinger Equation:
  - M. Hecht *et al.* PRD (2001).
- Chiral Quark Model:
  - K. Suzuki, W. Weise, NPA (1998).
  - D. Arndt, M. Savage, nucl-th (2001)
- Light-front constituent quark models:
  - Gerry Miller, *et al.* (too many to list).
- Instanton Model:
  - A. Dorokhov, L. Tomio, PRD (2000)
- QCD Sum Rule Calculations
  - A. Bakulev *et al.* PLB (2001).
- Lattice Gauge
  - C. Best *et al.* PRD (1997).

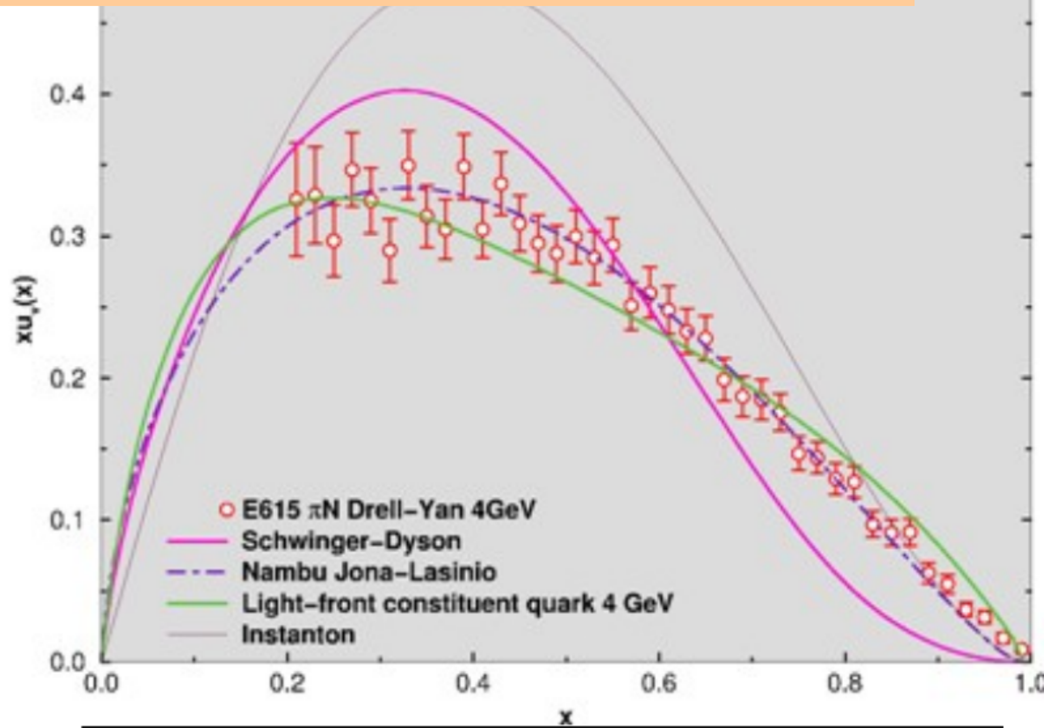

At some base q_0
NJL: $xq(x)/\ (1-x)^{\beta}$ $\beta = 1$
pQCD: $xq(x)/\ (1-x)^{\beta}$ $\beta = 2$
DSE: $xq(x)/\ (1-x)^{\beta}$ β ¼ 1.9
Evolution to experimental Q increases β.

Comparing theoretical predictions to phenomenological PDFs

- When fitting a nonperturbative model to cross section data is impractical, the model may be compared to the $\overline{MS}$ PDFs from a phenomenological set (CTEQ, JAM, NNPDF, etc.) constrained by the global QCD data
- The PDF is a theoretical construct, not a physical observable.
- For example, an unpolarized quark PDF in a hadron $A = p, n, \pi, K, \ldots$ in the $\overline{MS}$ factorization scheme is defined to all orders of α_s by

$$f_{q/A}(\xi,\mu) = \frac{1}{4\pi}\int_{-\infty}^{+\infty} dy^- \; e^{-i\xi p^+ y^-} \langle A|\bar{\psi}_q(0^+, y^-, \vec{0}_T)\gamma^+ W(A; y^-, 0)\psi_q(0^+, 0^-, \vec{0}_T\; |A\rangle$$

- QCD cross sections factorize in terms of PDFs $f_{a\backslash A}(\xi,\mu)$ and hard cross sections $\hat{\sigma}$. In Z production at the LHC:

$$\underbrace{\sigma_{pp\to\ell\bar{\ell}X}}_{\text{compared to experiment}} = \sum_{a,b=q,\bar{q},g} \int_0^1 d\xi_1 \int_0^1 d\xi_2\, \widehat{\sigma}_{ab\to Z\to\ell\bar{\ell}}\left(\frac{x_1}{\xi_1}, \frac{x_2}{\xi_2}; \frac{Q}{\mu}\right) f_{a/p}(\xi_1,\mu) f_{b/p}(\xi_2,\mu)$$

$$+\, \underbrace{\mathcal{O}\left(\Lambda_{QCD}^2/Q^2\right)}_{\text{power-suppressed correction}}$$

compared to experiment

power-suppressed correction

computed/evolved to N[x]LO in $\alpha_s(\mu)$

CT18 parton distributions

T.-J. Hou et al., arXiv:1912.10053

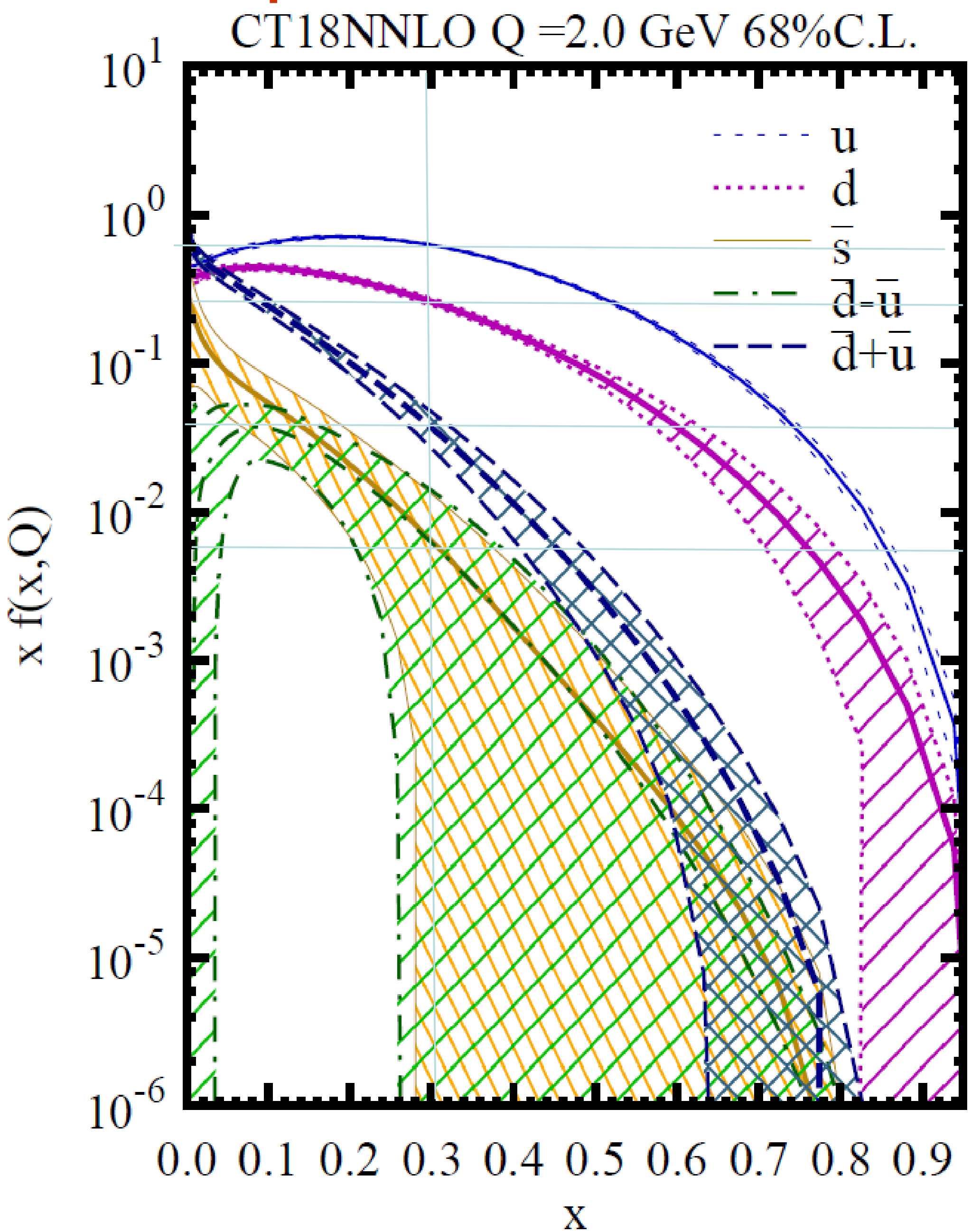

- Modern PDFs such as the CT18 (N)NLO PDF set are provided in the form of central fits and error sets for estimating 68% or 90% C.L. uncertainties
- Functional forms of some PDF sets at the initial scale Q_0 that may be motivated by nonperturbative models. Other sets use "unbiased" ultra-flexible functional forms given by neural networks.
- **Mimicry – a fundamental feature of multivariate optimization:**

Diverse functional forms of PDFs at the initial scale μ_0 provide equally good description of QCD data from DIS, Drell-Yan pair, jet, and $t\bar{t}$ production

Experimental data in CT18 PDF analysis

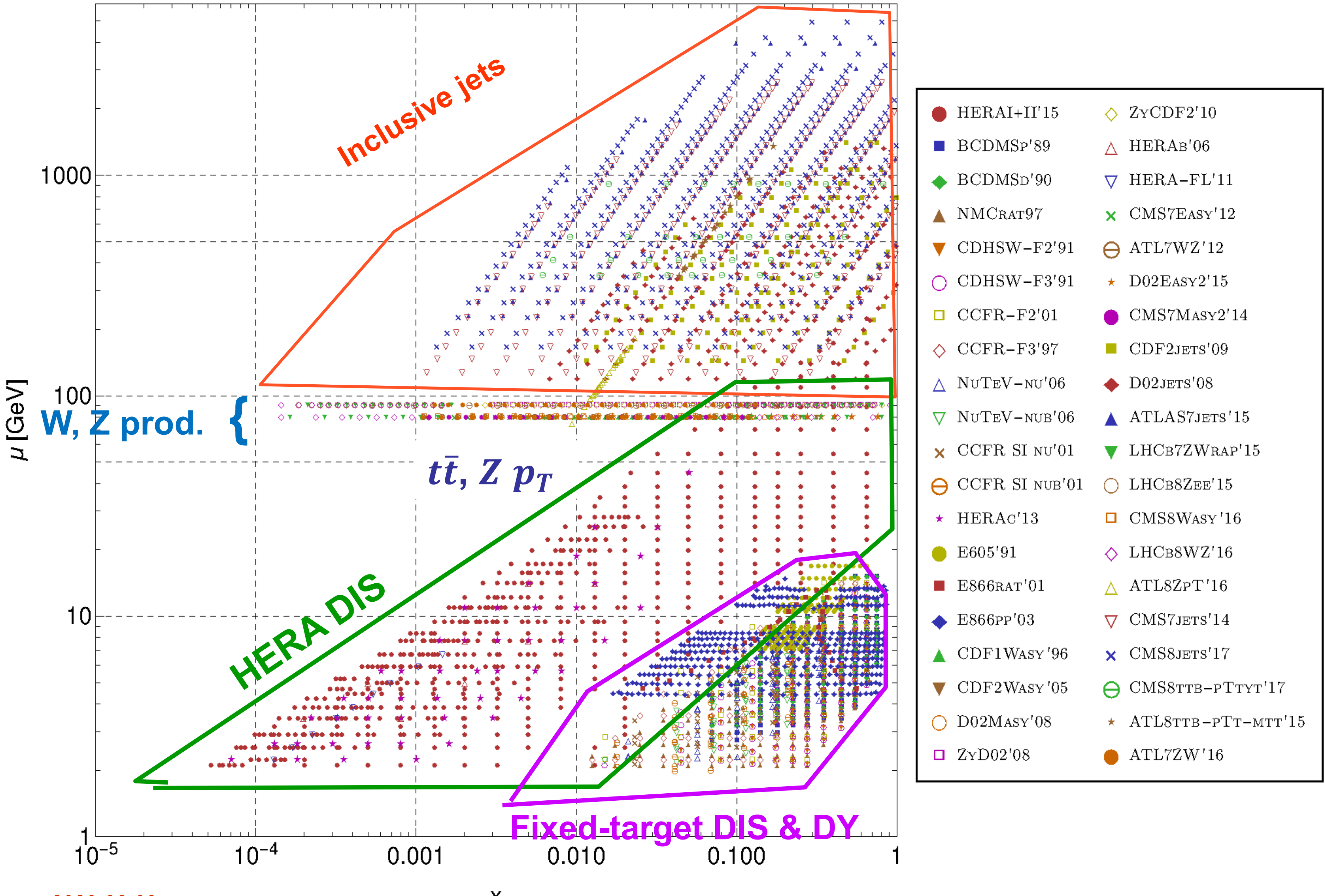

2020-06-03

Nadolsky, Olness, Courtoy, Hobbs,
Pion-Kaon Workshop @ JLab

Sources of the uncertainty on PDFs

1. **Experimental uncertainties**, e.g., statistical, correlated and uncorrelated systematic uncertainties of each experimental data set;
   – can be estimated using the $\Delta\chi^2 = 1$ criterion when experimental sets agree

2. **Theoretical uncertainties** due to the absent higher-order and power-suppressed radiative contributions, QCD scale choices, and uncertainties from using parton showering programs in experimental analyses
3. **Methodological uncertainties** associated with the selection of experimental data sets, fitting procedures, and goodness-of-fit criteria.
4. **Parameterization uncertainties** associated with the choice of the PDF functional form;
   – contribute at least a half of the CT18 total PDF uncertainty
   – **Rapid variations in $f_{a/A}(\xi, \mu)$ are generally not constrained well**

The uncertainty of published CT18 PDFs estimates the sum of four contributions

Kovarik et al., arXiv: 1905.06957

"Error sets" for computing PDF uncertainties

1. Based on diagonalization of the Hessian matrix (CTEQ, MMHT, ABM, HERAPDF, ...)
   - PDFs at the initial scale Q_0 are given by polynomial functional forms,

$$f(\xi, Q_0) = A_0\, x^{A_1}(1-x)^{A_2} P(x; A_3, A_4 \ldots)$$

2. Based on Monte-Carlo sampling of probability and neural networks (NNPDF)
   - The $x^{A_1}(1-x)^{A_2}$ dependence is modulated by a neural network function $P_{NN}(x)$ that can oscillate
   - A nonpert. model can predict such replicas in an x-averaged sense

See, e.g., Nocera, 1410.7290; Ball, Nocera, Rojo, 1604.00024

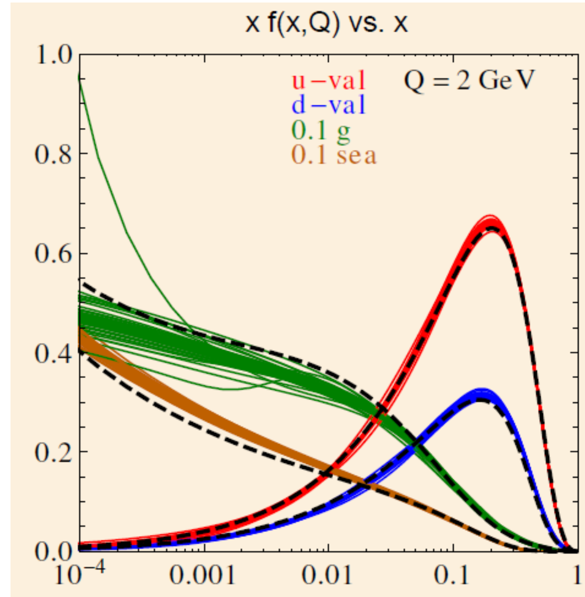

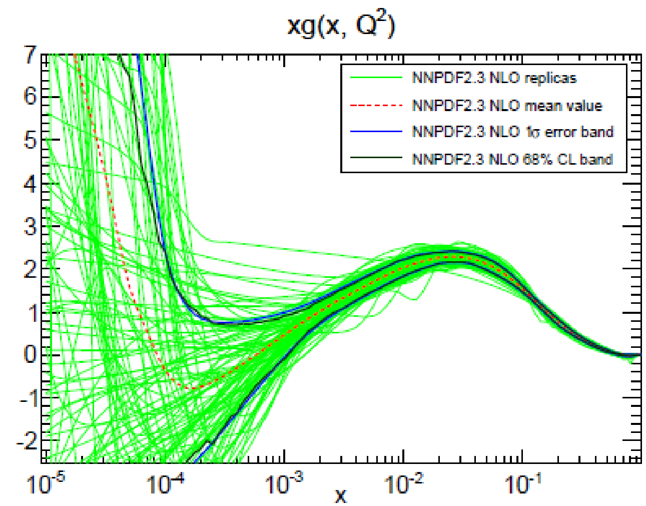

Example: the effective $(1-x)^{A_2}$ dependence of nucleon and pion PDFs

Drell, Yan, West, PRL 24 (1970) 1206
Ezawa, Nuovo Cim., A23 (1974) 271
Farrar, Jackson, PRL, 35 (1975) 1416
Berger, Brodsky, PRL 42, 940
Brodsky, Lepage, 1979
and many others

Counting rules for a quark distribution with $x \to 1$ in a hadron A moving with $p^+ \gg 1\ GeV$, with dependence on helicities:

$$\lim_{x\to 1} f(x, \mu_0 \sim 1\ GeV, \lambda_q) \propto (1-x)^{2\,n_s - 1 + 2|\lambda_q - \lambda_A|}$$

n_s is the number of spectator fermions, λ_q and λ_A are helicities of struck quark and hadron A

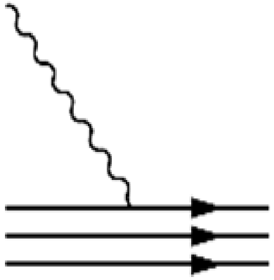

Nucleon valence PDFs: $n_s = 2,\ \lambda_A = \pm\frac{1}{2}, \left|\lambda_q - \lambda_A\right| = 0\ or\ 1$;

$$\lim_{x\to 1} \sum_{\lambda_q,\lambda_A} f_{q/p}(x, \mu_0, \lambda_q) \propto (1-x)^{A_2} \text{ with } \mathrm{A}_2 = 3$$

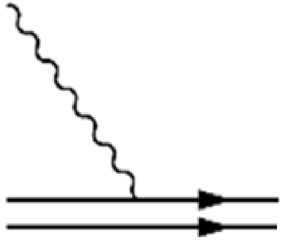

Pion valence PDFs: $n_s = 1,\ \lambda_A = 0,\ |\lambda_q - \lambda_A| = 1$;

$$\lim_{x\to 1} \sum_{\lambda_q,\lambda_A} f_{q/\pi}(x, \mu_0, \lambda_q) \propto (1-x)^{A_2} \text{ with } A_2 = 2$$

- A_2 is the same for u and d quarks
- At $\mu > \mu_0$, the effective A_2 increases because of DGLAP evolution

Do phenomenological PDFs agree with Brodsky-Farrar quark counting rules?

Note: the PDF parametrizations are complex. See CT18 parametrizations in the backup. We will examine 363 CT18 candidate parametrization forms.

If at $x \to 1$:

$$f(x, Q_0) = \underbrace{(1-x)^{A_2^{true}}}_{fast\ function} \times \underbrace{\Phi(x)}_{slow\ function} ,$$

then

$$A_{2,eff}(x) \equiv \frac{\partial \ln\big(f(x, Q_0)\big)}{\partial \ln(1-x)} \approx A_2^{true} + small\ term.$$

parametric forms in CT18

Full description in arXiv:1912.10153

form for u_v, d_v

$$q_v(x, Q = Q_0) = x^{a_1 - 1}(1 - x)^{a2}\, P^v_a(y) \qquad y \equiv \sqrt{x}$$

$$P^v_a(y) = a_3(1-y)^4 + a_4 4y(1-y)^3 + a_5 6y^2(1-y)^2 + a_6 4y^3(1-y) + y^4$$

$$a_6 = 1 + \frac{1}{2}a_1$$

- more flexible form (i.e., high-order polynomial) used for SU(2) sea PDFs; e.g.:

$$\bar{d}(x, Q = Q_0) = x^{a_1 - 1}(1 - x)^{a2}\, P^{\bar{d}}_a(y)$$

$$P^{\bar{d}}_a(y) = a_3(1-y)^5 + a_4 5y(1-y)^4 + a_5 10y^2(1-y)^3$$
$$+ a_6 10y^3(1-y)^2 + a_7 5y^4(1-y) + y^5$$

Effective $(1-x)^{A_2}$ dependence, **proton**

$$A_{2,eff}(x) \equiv \frac{\partial \ln\big(f(x,Q_0)\big)}{\partial \ln(1-x)}$$

is computed at $Q = 1.3, 2, 10$ GeV; and x=0.85, 0.5, 0.3.

The scatter points are for 363 distinct parametric forms of CT18 NNLO candidates.

3679 data points in the fit, variation in χ^2 is within 100 units for the shown fits

The fitted data are below $x = 0.75$. Extrapolation to $x = 0.85$.

CT18 NNLO candidates, effective (1-x) powers for valence quarks in the nucleon

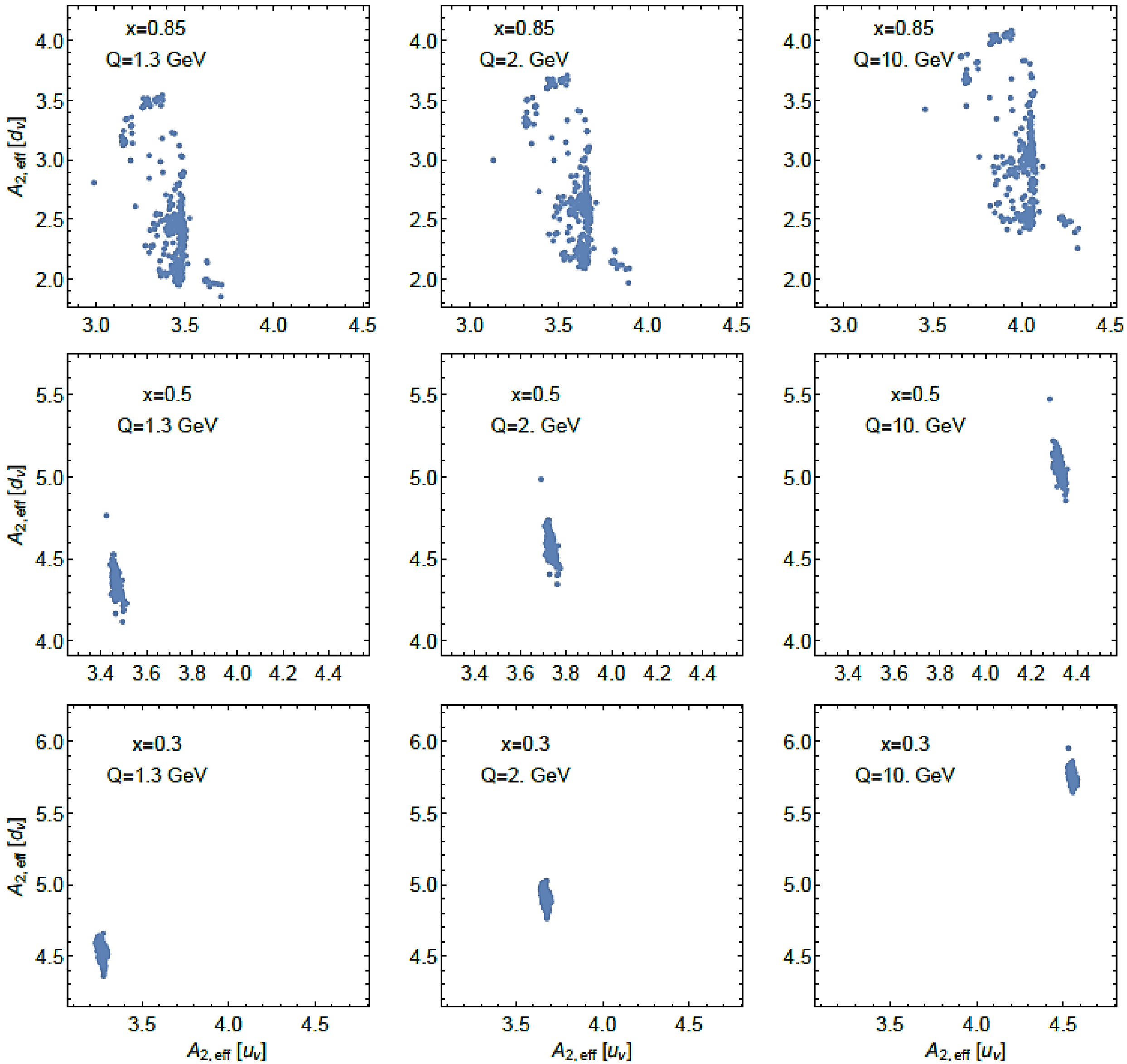

Figure: A. Courtoy, PN

Effective $(1-x)^{A_2}$ dependence, **proton**

x=0.85, $Q = Q_0 = 1.3$ GeV:
$A_{2,eff}$ ≈3-4 for u_{val}, 2-4 for d_{val}

$A_{2,eff}$ increases with Q

$x = 0.5$ and 0.3: ;larger $A_{2,eff}(d_{val})$, stronger DGLAP evolution

∴ Uncertainty $\delta A_{2,eff}$ of order 0.5 (2) units for u_{val} (d_{val}) due to parametrization dependence

CT18 NNLO candidates, effective (1-x) powers for valence quarks in the nucleon

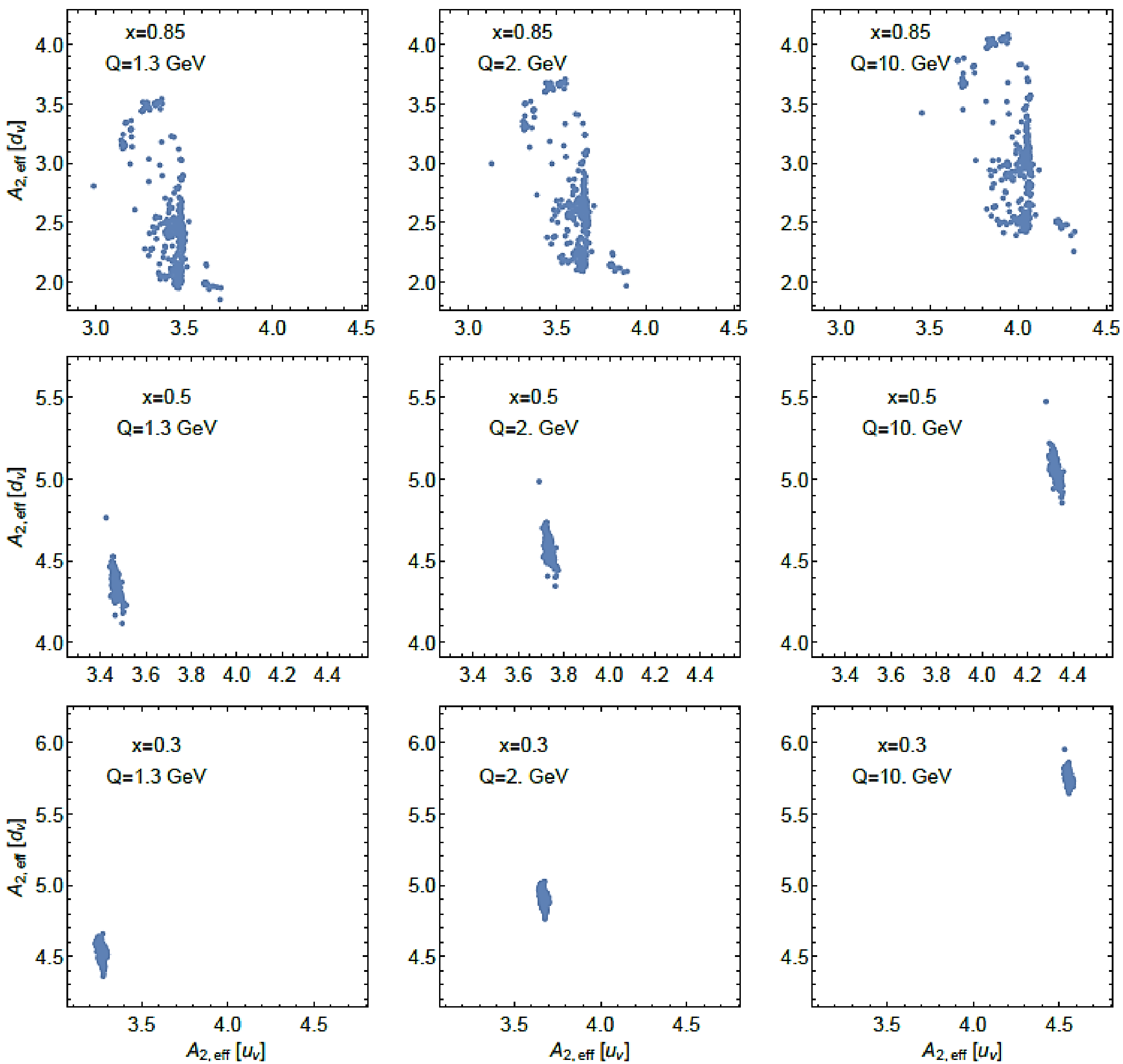

Figure: A. Courtoy, PN

Effective $(1-x)^{A_2}$ dependence, **pion**

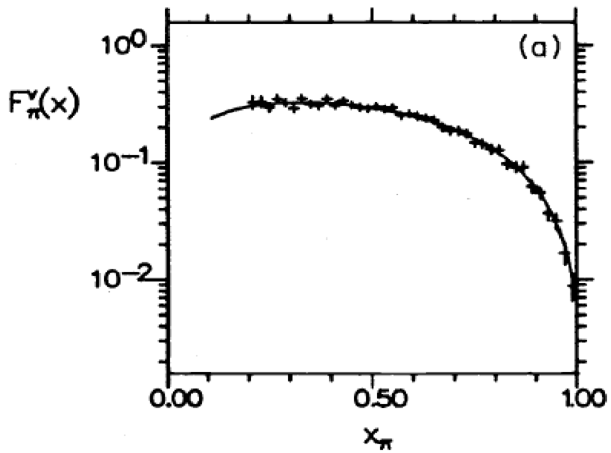

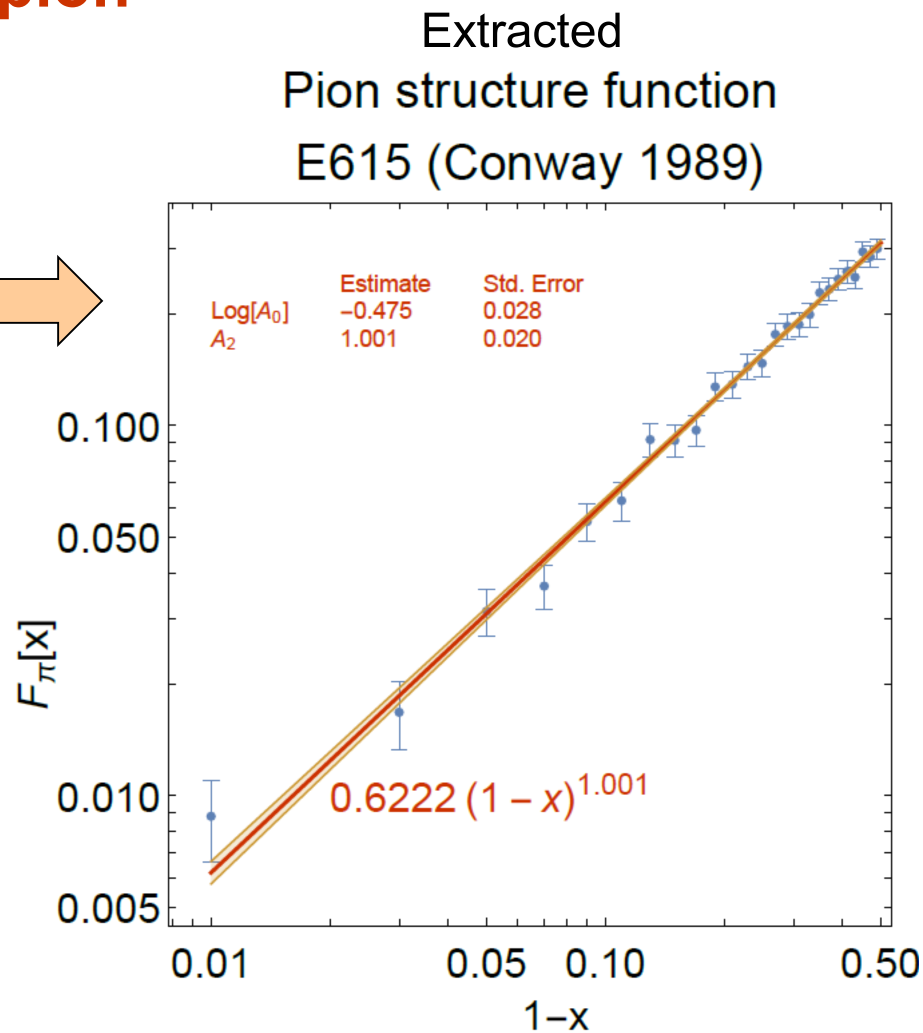

The pion DY data from the E615 experiment, and the derived LO pion structure function $F_\pi(x) = xv(x)$, agree exceptionally with $v(x) \propto (1-x)$ at $x > 0.5$.

Right: a linear fit of $\ln(xF_\pi(x))$ vs. $\ln(1-x)$ in Mathematica gives $A_{2,eff} = 1.001 \pm 0.020$ – with unusual precision!

Does this observation rule out the $(1-x)^2$ dependence?

Effective $(1-x)^{A_2}$ dependence, **pion**

Mimicry I

Very similar PDFs can be obtained using distinct functional forms

xFitter Pion NLO PDFs, arXiv:2002.02902

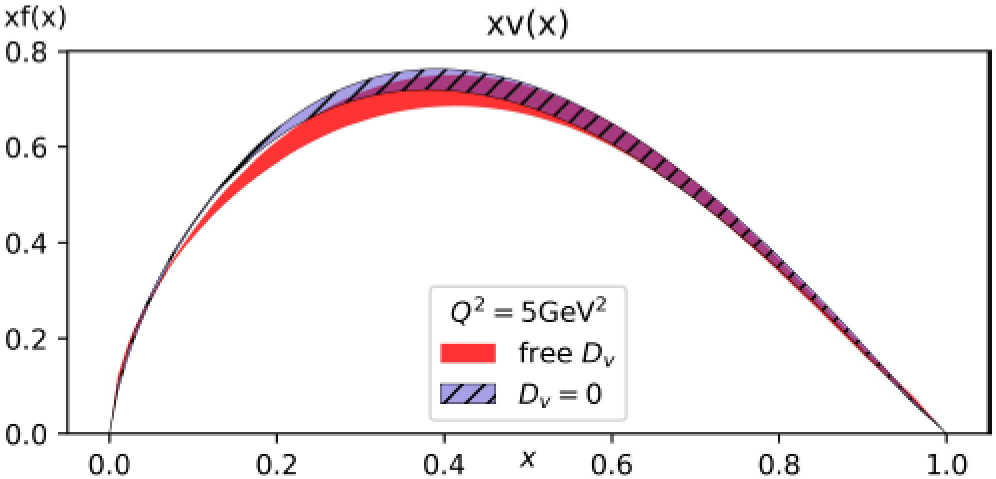

FIG. 2. The valence distribution when using minimal parameterisation ($D_v = 0$) and the extended parameterisation with free D_v. The shown uncertainty bands do not include scale variations. The high-x behavior is linear in $(1-x)$.

1. $D_v = 0$ fit at Q_0:
   $xv_1(x) = 2.60\ x^{0.75}\ (1-x)^{\mathbf{0.95}}$
2. Free D_v fit at Q_0:
   $xv_2(x) = 1.72\ x^{0.63}\ (1-x)0.26\ (1-x^{5/2})$

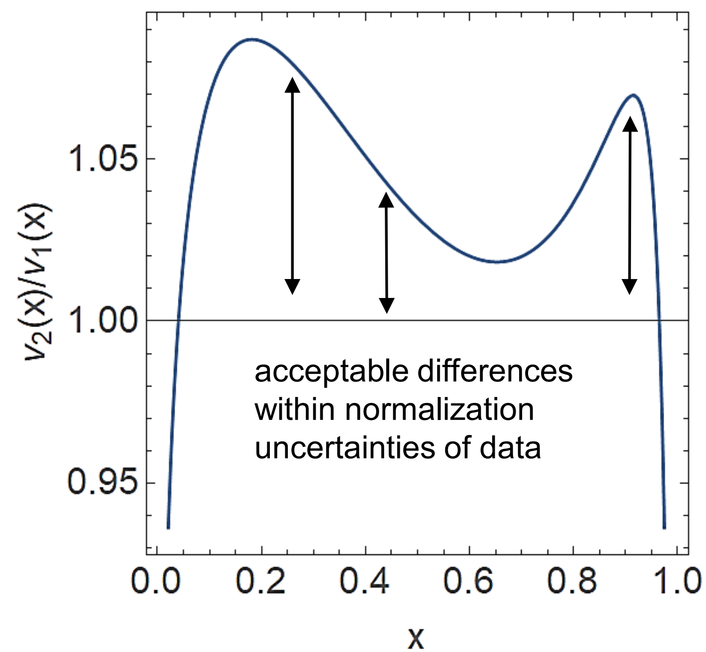

$$\lim_{x\to 1} \frac{v_1(x)}{v_2(x)} = 21.6\,(1-x)^{0.69} + \cdots$$

Effective $(1-x)^{A_2}$ dependence, **pion**

Mimicry II

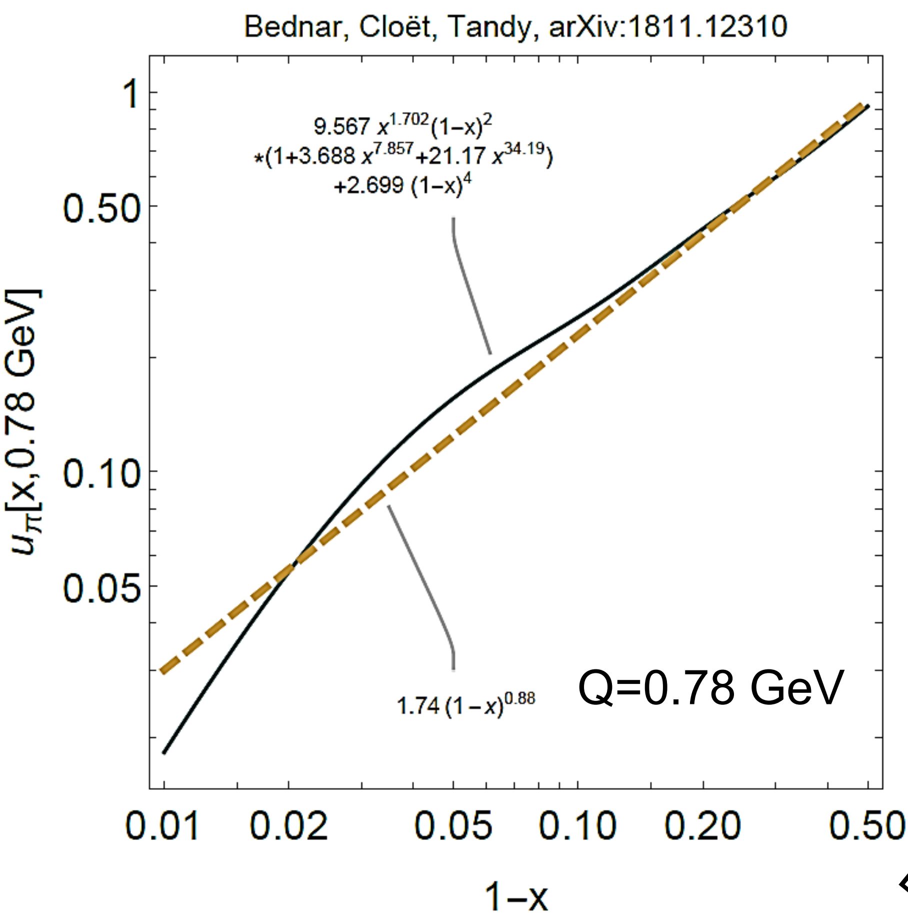

Bednar, Cloët, Tandy, 2018

Predict pion PDFs from a truncated DSE approach at low scale $Q = 0.78$ GeV,

$xv(x) = A_0(1-x)^2 \times [fancy\ polynomial]$
$\quad +c_4(1-x)^4$

The form at Q=0.78 GeV is quantitatively close to

$$xv(x) = 1.74\ (1-x)^{0.88};$$

evolves to $xv(x)$ that is nearly linear in $(1-x)$ in the DY data region, agrees with JAM PDFs

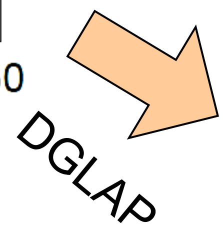

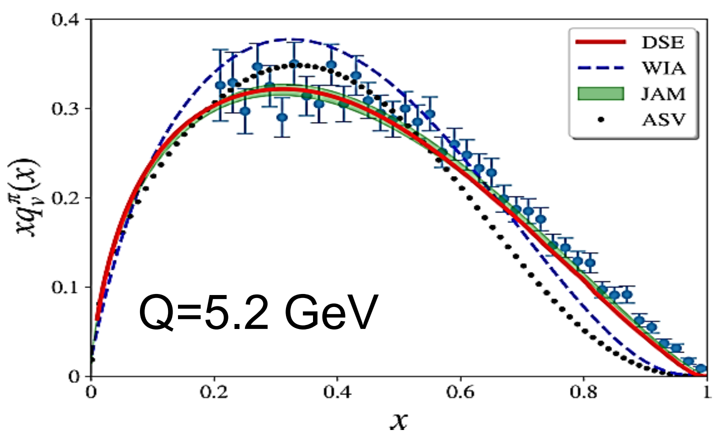

Pion PDFs at $\zeta_5 = 5.2$ GeV

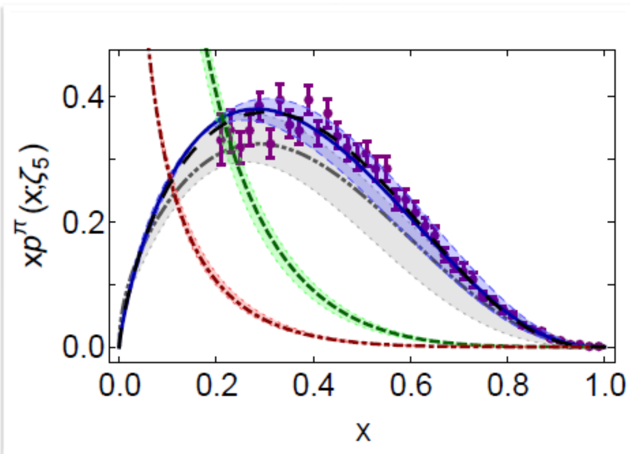

- Solid (blue), $q^{\pi}(x;\zeta_5)$

$$q^{\pi}(x) = n_{q^{\pi}}\, x^{\alpha}(1-x)^{\beta}[1+\rho\, x^{\alpha/4}(1-x)^{\beta/4}+\gamma\, x^{\alpha/2}(1-x)^{\beta/2}]$$

- Long-dashed (black), DSE in 2001 — Hecht et al.. Phys. Rev. C 63, 025213 (2001)
- Dot-dot-dashed (grey), Lattice QCD — Raza Sabbir Sufian et al.. Phys. Rev. D 99, 074507 (2019)
- Data (purple) from — J.S.Conway et al.. Phys. Rev. D 39 (1989) 92-122
- Rescaled analysis — Matthias Aicher et al.. PRL 105, 252003 (2010)

	$n_{q^{\pi}}$	α	β	ρ	γ
	7.81	-0.153	2.54	-1.20	0.505
ζ_5	7.28	-0.169	2.66	-1.21	0.531
	6.48	-0.188	2.78	-1.19	0.555

$\beta(\zeta_5) = 2.66(12)$

- Agree with Lattice QCD $\beta_{\text{lQCD}}(\zeta_5) = 2.45(58)$

- Low-order moments in comparison with Lattice QCD

ζ_5	$\langle x\rangle_u^{\pi}$	$\langle x^2\rangle_u^{\pi}$	$\langle x^3\rangle_u^{\pi}$
Ref. [31]	0.17(1)	0.060(9)	0.028(7)
Herein	0.21(2)	0.076(9)	0.036(5)

- Dashed (green), gluon; Dot-dashed (red), sea-quark.
- First Moment $\langle x\rangle_g^{\pi} = 0.45(1)$, $\langle x\rangle_{\text{sea}}^{\pi} = 0.14(2)$.

22

☺ M. Ding shows that pion DY data are compatible with the form

$$q_{\pi}(x) = A_0 x^{-0.153}(1-x)^{2+\epsilon} \times [fancy\ polynomial]$$

☹ It is often unclear how well individual models agree with the data. Do they have good χ^2, are there systematic disagreements in some kinematic regions?

⇒ **Good fits must pass multiple statistical tests**, see *Kovarik, PN, Soper*, [1905.06957]

QCD scale dependence in the Drell-Yan process

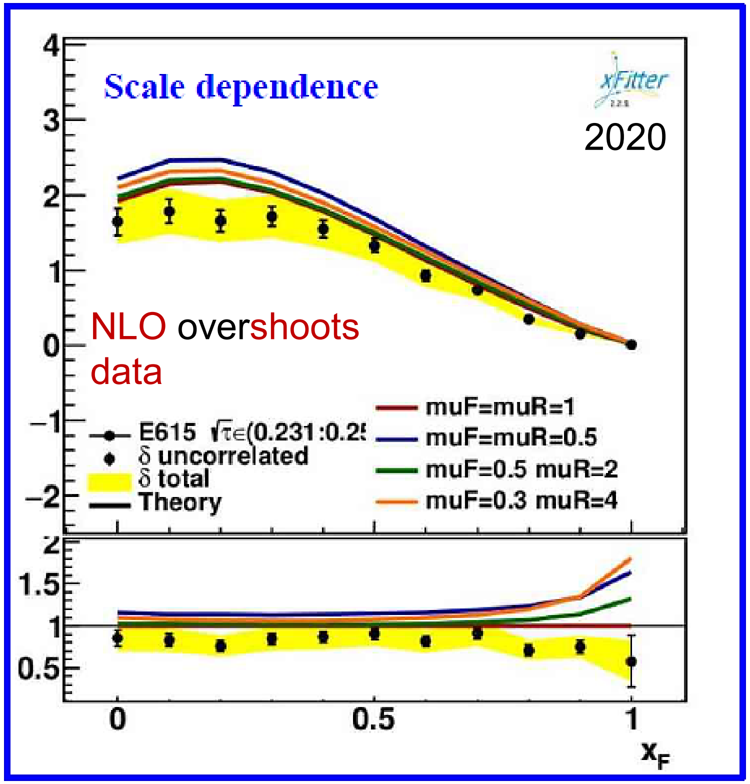

Factorization scale dependence of Drell-Yan cross sections is generally mild at NLO, but grows toward largest x values.

At $x \gtrsim 0.5$, NLL threshold resummation:

- reduces the scale dependence
- increases A_2 from 1 at NLO with $\mu = M_{\ell\bar{\ell}}$ to 2.34
- no large $\ln(1-x)$ terms evident at smaller x

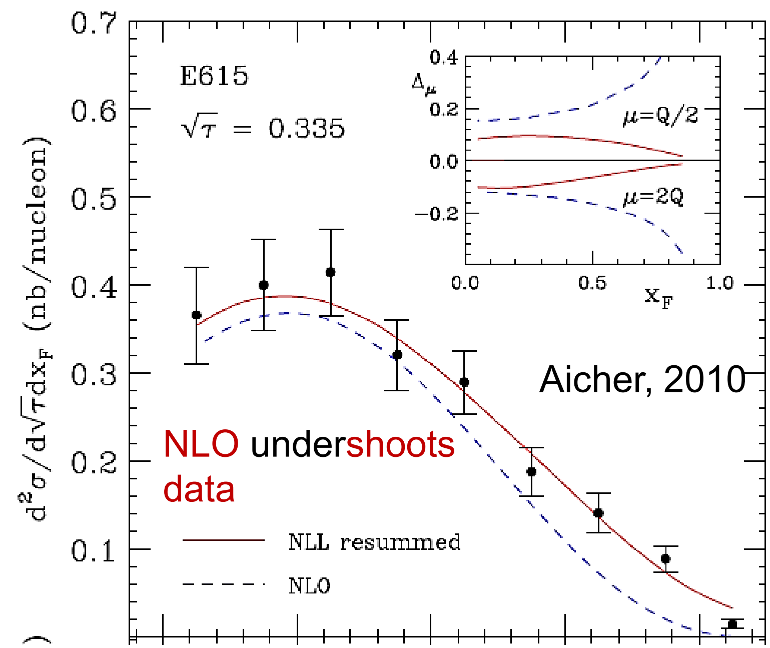

Instructive to repeat the NLL resummation calculation by Aicher, Shäfer, Vogelsang (2010) at NNLO with **complete studies of uncertainties due to matching, nonpert. contributions, nuclear PDFs, and correlation with overall normalization**

Threshold resummation for DY process

Aicher, Shafer, Vogelsang, arXiv:1009.2481, and references therein

When $z \equiv \frac{Q^2}{\hat{s}} \to 1$:

$$\frac{d\sigma}{dQ^2 d\eta} = \int_{-\infty}^{\infty} \frac{dM}{2\pi} e^{-iM\eta} \int_{C-i\infty}^{C+i\infty} \frac{dN}{2\pi i} \tau^{-N} \sigma(N, M). \quad \equiv W$$

$$\sigma(N, M) = \sigma_0 \sum_{a,b} f_a^{\pi, N+i\frac{M}{2}} f_b^{A, N-i\frac{M}{2}} \tilde{\omega}_{ab}(N, M).$$

$$\ln \tilde{\omega}_{q\bar{q}} = C_q \left(\frac{Q^2}{\mu^2}, \alpha_s(\mu^2) \right) + 2 \int_0^1 d\zeta \frac{\zeta^{N-1} - 1}{1 - \zeta} \times \int_{\mu^2}^{(1-\zeta)^2 Q^2} \frac{dk_\perp^2}{k_\perp^2} A_q(\alpha_s(k_\perp)),$$

where $\widetilde{\omega}_{ab}$ resum the soft and collinear gluon contributions:

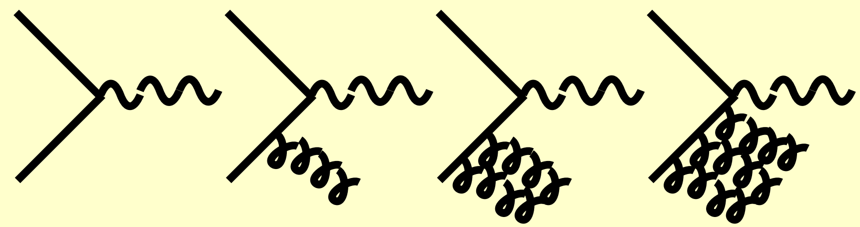

The resummed W term dominates when $\log(1 - z)$ terms are large.
In the kinematics of pion DY data, typical $z \ll 1$, the full description requires matching the W term on the fixed-order (**FO**) cross section at (N)NLO in α_s:

All z: $\boldsymbol{\frac{d^2\sigma}{dQ^2 d\eta} = W + FO - overlap}$

Final remarks

1. A theoretical model cannot be falsified empirically if its uncertainty is unknown.

2. Multiple functional forms of PDFs adequately describe the global set of experimental data.

3. The x −dependence of the best-fit PDF depends on the PDF definition (e.g., $\overline{MS}$ factorization scheme), order of α_s, treatment of power-suppressed corrections, and other factors. Comparison to the pheno PDF requires proper conversion into the definition adopted by the pheno PDF.

4. Threshold resummation may modify both the shapes and normalizations of some pion DY cross sections. The resummed W term dominant at $Q^2/\hat{s} \to 1$ must be matched to the fixed-order (FO) cross section at $Q^2/\hat{s} < 1$. The resulting PDFs may depend on the resummed nonpertubative contributions at large Mellin moments N and the matching procedure.

5. Determination of sea quark and gluon PDFs in the pion generally benefits from the extended reach in Q in DIS and other processes.

Thank you
for your attention

parametric forms in CT18

Full description in arXiv:1912.10153

form for $u_v,\ d_v$

$$q_v(x, Q = Q_0) = x^{a_1 - 1}(1-x)^{a2}\, P_a^v(y) \qquad y \equiv \sqrt{x}$$

$$P_a^v(y) = a_3(1-y)^4 + a_4 4y(1-y)^3 + a_5 6y^2(1-y)^2 + a_6 4y^3(1-y) + y^4$$

$$a_6 = 1 + \frac{1}{2} a_1$$

- more flexible form (i.e., high-order polynomial) used for SU(2) sea PDFs; e.g.:

$$\bar{d}(x, Q = Q_0) = x^{a_1 - 1}(1-x)^{a2}\, P_a^{\bar{d}}(y)$$

$$P_a^{\bar{d}}(y) = a_3(1-y)^5 + a_4 5y(1-y)^4 + a_5 10y^2(1-y)^3 + a_6 10y^3(1-y)^2 + a_7 5y^4(1-y) + y^5$$

parametric forms in CT18

form for u_v, d_v

$$q_v(x, Q = Q_0) = x^{a_1 - 1}(1-x)^{a_2} P_a^v(y) \qquad y \equiv \sqrt{x}$$

cent. fitted parameter, **CT18**	u_v	d_v	g	$\bar{u}$	$\bar{d}$	s
a_1	0.7632	0.7632	0.5310	−0.0219	−0.0219	−0.0219
a_2	3.0361	3.0361	3.1481	7.7366	7.7366	10.3099
a_3	1.5019	2.6141	3.0314	(4)	(4)	(4)
a_4	−0.1467	1.8275	−1.7049	0.6179	0.2922	0.4660
a_5	1.6711	2.7203	—	0.1949	0.6470	0.4660
a_6	—	—	—	0.8709	0.4749	0.2253
a_7	—	—	—	0.2667	0.7414	0.2253
a_8	—	—	—	0.7332	—	(1)

cent. fitted parameter, **CT18Z**	u_v	d_v	g	$\bar{u}$	$\bar{d}$	s
a_1	0.7867	0.7867	0.2892	0.0096	0.0096	0.0096
a_2	3.1480	3.1480	1.8720	8.2730	8.2730	11.3771
a_3	1.5586	3.5016	3.5377	(4)	(4)	(4)
a_4	−0.0750	1.8654	−1.6654	0.6791	0.2999	0.6531
a_5	1.6052	3.5986	—	−0.0016	0.5322	0.6531
a_6	—	—	—	1.0851	0.7533	0.0539
a_7	—	—	—	0.0455	0.4404	0.0539
a_8	—	—	—	0.7592	—	(1)

$$P_a^{\bar{d}}(y) = a_3(1-y)^5 + a_4 5y(1-y)^4 + a_5 10y^2(1-y)^3 + a_6 10y^3(1-y)^2 + a_7 5y^4(1-y) + y^5$$

Explore various non-perturbative parametrization forms of PDFs

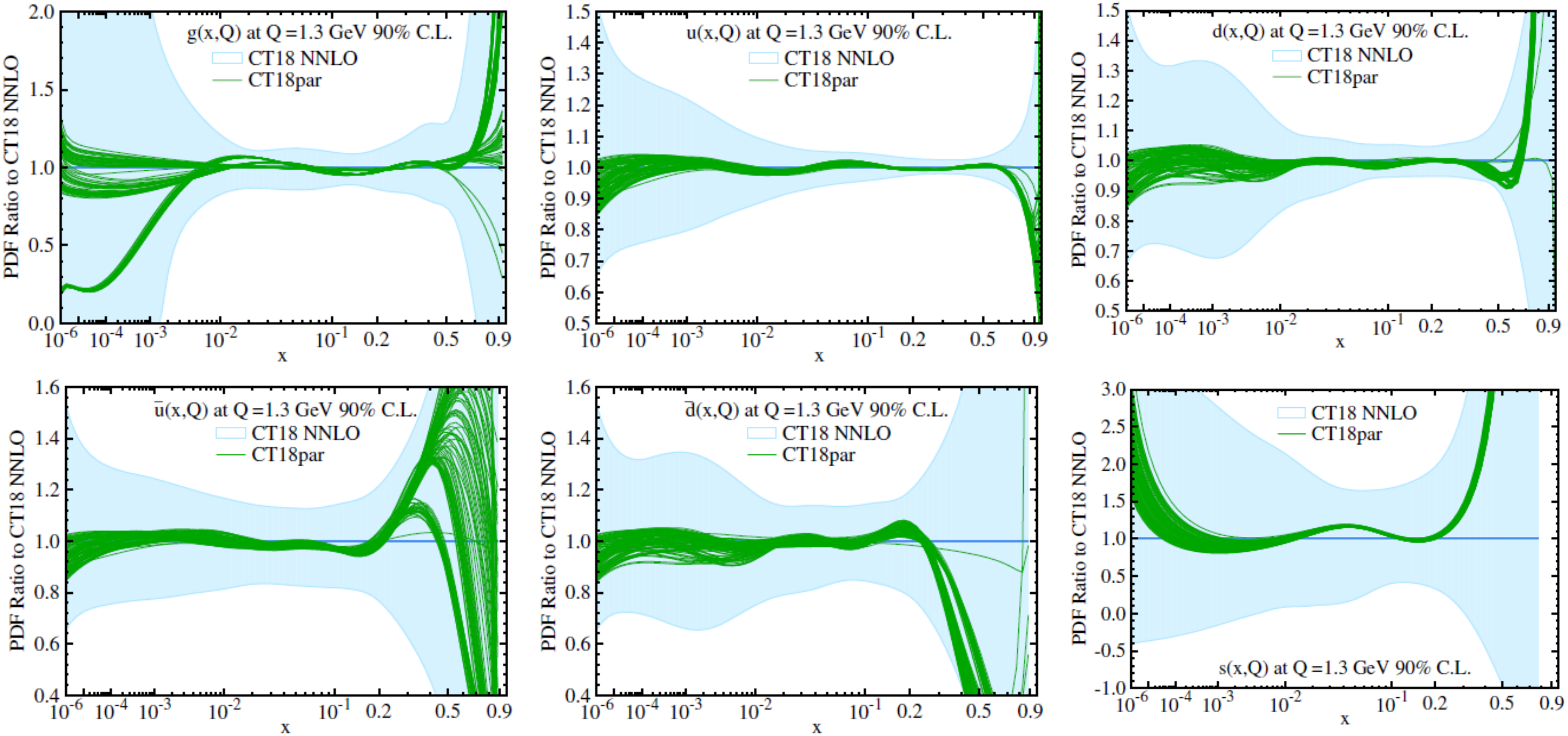

- CT18par – a sample of **some** non-perturbative parametrization forms tried in CT18
- No data constrain very large x or very small x regions.